Eur Biophys J (2008) 37:205–212
DOI 10.1007/s00249-007-0217-4

ORIGINAL PAPER

Photoacoustic spectroscopy of aromatic amino acids in proteins

Milton Roque Bugs · Raquel Kely Bortoleto-Bugs · Marinônio Lopes Cornélio

Received: 26 March 2007 / Revised: 14 August 2007 / Accepted: 24 August 2007 / Published online: 6 September 2007

Abstract This paper concerns the use of photoacoustic spectroscopy (PAS) to study the presence of aromatic amino acid in proteins. We examined the aromatic amino acids in six proteins with well-known structures using absorption spectra of near ultraviolet PAS over the wavelength range 240–320 nm. The fundamental understanding of the physical and chemical properties that govern the absorption of light and a subsequent release of heat to generate a transient pressure wave was used to test the concept of monitoring aromatic amino acids with this method. Second derivative spectroscopy in the ultraviolet region of proteins was also used to study the regions surrounding the aromatics and the percentage area in each band was related in order to determine the contribution in function of the respective molar extinction coefficients for each residue. Further investigation was conducted into the interaction between sodium dodecyl sulphate (SDS) and bothropstoxin-I (BthTx-I), with the purpose of identifying the aromatics that participate in the interaction. The clear changes in the second derivative and curve-fitting procedures suggest that initial SDS binding to the tryptophan located in the dimer interface and above 10 SDS an increased intensity between 260 and 320 nm, demonstrating that the more widespread tyrosine and phenylalanine residues contribute to the SDS/BthTx-I interactions. These results demonstrate the potential of near UV-PAS for the investigation of membrane proteins/detergent complexes in which light scattering is significant.

Keywords Photoacoustic spectroscopy · Aromatic amino acids · Curve-fitting · Bothropstoxin-I · SDS

M. R. Bugs · R. K. Bortoleto-Bugs
COGNITUS Project, CENPES/PETROBRAS,
Rio de Janeiro, RJ, Brazil

M. R. Bugs (✉) · R. K. Bortoleto-Bugs
CenPRA, Centro de Pesquisas Renato Archer,
Rodovia Dom Pedro I, km 143,6, Bairro Amarais,
CEP 13069-901 Campinas, SP, Brazil
e-mail: milton.bugs@cenpra.gov.br

M. L. Cornélio
Departamento de Física, IBILCE/UNESP,
Sao Jose do Rio Preto, SP, Brazil

Introduction

The biological macroscopic world is controlled by interactions that occur at the molecular level and indeed in biological systems, the processes are released by enzymes that have an infinite combination of the amino acids. So it is very important to understand the vast possibilities of interactions between these residues, as well as the elucidation of the mechanism in the interaction processes which are always managed by a determined sequence of amino acid for each protein, providing guidelines and clarifying the mechanism created and refined by nature in the evolution process while keeping the better part of the function. Along this line of knowledge, the aromatic amino acids remain an interesting object of study in order to aid our understanding of these mechanisms. In the hierarchic view, studies of the relationship between known structures and new spectroscopic techniques provide conceptual and practical approaches to the elucidation of the action of the molecular mechanism of a biologically active enzyme.

Conventional ultraviolet spectroscopy of aromatic amino acids is a rich source of information, mainly with regard to structural changes in proteins. Techniques such as absorbance and fluorescence spectroscopy have been extensively

used in the characterization of structural changes in proteins in a wide variety of physicochemical contexts. Although these techniques are extremely useful tools for the investigation of protein function, they have proven to be of limited utility in the investigation of membrane proteins due to the errors induced by the high levels of light scattering that are typically encountered in mixtures of membrane proteins associated with amphiphilic molecules. The effect of intense light scattering, which seems to be a curse on the experimental investigation of amphiphilic proteins, is in fact a clear clue to a more detailed model in the description of the system. Therefore, the application of a technique that combines the benefits of ultraviolet aromatic spectroscopy with minimal artifacts from light scattering would be highly useful for the study of membrane proteins.

The state of the art in applying Photoacoustic Spectroscopy (PAS) has a wide application in the study of biological events such as photosynthesis (Malkin and Cahen 1979; Fork and Herbert 1993), electron transfer (Cornélio and Sanches 1994, 1995), protein analysis (Kurian et al. 1997; Bugs et al. 2007), protein folding (Abbruzzetti et al. 2000), and quantum yield (Adams et al. 1977, 1980; Lahmann and Ludewig 1977; Quimby and Yen 1980; Mandelis 1982), as well as in the determination of the non-radiative relaxation processes of DNA-dye binding studies (Bugs and Cornélio 2001, 2002). PAS (Rosencwaig 1980) is derived from the photoacoustic (PA) effect and is an optical spectroscopy technique. Due to the non-radiative relaxation of excited molecules, absorbed energy is converted partially into heat, which generates a pressure wave that is detected by a sensitive microphone located in the compartment of the sample. Generally, due to its versatility, PAS should be applied to problems, which cannot be solved by conventional spectroscopic methods; however, its application in the study of biological materials has been limited to samples, which absorb strongly in the visible range 400–600 nm. Indeed, it has recently been demonstrated that PAS is useful for monitoring the interaction between drugs and DNA (Bugs and Cornélio 2001, 2002), and in a recent study with a complete characterization of the thermodynamics governing DNA intercalation with and without stretching forces (Vladescu et al. 2005) confirming reasonable agreement with our PAS results. We previously obtained additional insights into the formation and dynamics of the interaction of SDS with bothropstoxin-I (BthTx-I) using a novel configuration of near UV-PAS to investigate the microenvironments of aromatic residues, demonstrating the capacity of this method to identify distinct binding modes of SDS to the protein which are not readily detectable by other techniques (Bugs et al. 2007). The present study is part of an ongoing effort in our laboratory with the objectives of demonstrating the feasibility of PAS in the near ultraviolet region (240–320 nm) for the detection of aromatic amino acids in proteins, and of applying the technique as a spectroscopic method in biophysical problems, in order to gain novel insights into biological questions.

The aim of this experiment is the analysis of the applicability of PA measurements in investigating aromatic amino acids in proteins and quantifying the fractional contribution of each aromatic in the protein spectrum, as well as in understanding some changes in the protein structure. Under these conditions, we used a configuration of near UV-PAS (Bugs et al. 2007) to investigate a set of known proteins and also to accompany and quantify the changes in the microenvironments of the aromatic residues on titration of the BthTx-I with sodium dodecyl sulphate (SDS).

Materials and methods

Protein purification and sample preparation

Bothropstoxin-I (BthTx-I), a Lys49-PLA_2 isolated from the venom of *Bothrops jararacussu* was purified using a combination of cation-exchange and size exclusion chromatography as previously described (Bortoleto-Bugs et al. 2004); Lysozyme (LYS) (GE Healthcare Bio-Sciences) and β-Lactoglobulin A (LGA), Bovine serum albumin (BSA), Rabbit serum albumin (RSA) and Ovalbumin (OVA) (Sigma Aldrich), were used without further purification. Protein purity was routinely evaluated by silver staining of SDS-PAGE gels, and stored at 4°C. For spectroscopic analyses, the protein samples were prepared in 25 mM Tris–HCl buffer at pH 7.0 with 150 mM of NaCl at final protein concentrations of 2 mM and the titration's of SDS on BthTx-I varied from 0 to 28 mM.

Photoacoustic measurements

The PA spectrometer was constructed in our laboratory and the details of this have been previously presented (Bugs and Cornélio 2001). For the PA measurements in the near UV region (240–320 nm), a closed cylindrical steel cell with a quartz window equipped with a highly sensitive condenser microphone was used. A monochromatic light source consisting of a light housing with a 300 W xenon arc lamp produced a single and continuous beam that was modulated by a mechanical chopper at 10 Hz. The microphone signal was registered with a lock-in amplifier and transferred to a computer via a COM interface. The volume of the gas in the cell was 1 cm^3, and the thickness of the sample was 2 mm when the cell contained 200 µl of liquid sample. The addition of SDS to the BthTx-I solution

was performed using a Hamilton microliter syringe in order to ensure precise control of the concentration and volume of the sample, and during the titration of the SDS, the sample volume was maintained at 200 µl. All measurements were performed at 25°C, and each point in the spectrum is the average of 50 data collection repetitions. All PAS experiments were repeated at least three times and the normalization of the spectra was performed using the PA spectrum of black carbon (Rosencwaig 1980).

Photoacoustic data analysis

Absorbance of the modulated light that impinges on the sample results in modulated heat generation, which after diffusion to the sample surface, generates a modulated pressure signal in the transfer gas inside the PA cell. The PA signal depends inversely on the modulation frequency of the light, and may be represented as a vector with amplitude and phase characteristics. The amplitude signal is proportional to the amount of light absorbed, which depends on the optical absorption coefficient, $\beta = 2.303\varepsilon C$, where ε is the molar extinction coefficient and C is the concentration (Perkampus 1992). Thus, the PA amplitude signal, measured from 240 to 320 nm reflects the absorbance of the aromatic amino acid species: $A_{PAS} = \varepsilon_W C_W + \varepsilon_Y C_Y + \varepsilon_F C_F$, where $\varepsilon_{W,Y,F}$ represent the respective molar extinction coefficients for each amino acid (W, tryptophan; Y, tyrosine and F, phenylalanine), and $C_{W,Y,F}$ represents the numbers of each aromatic amino acid. The molar extinction coefficients of the substance also depends on the wavelength (λ) of the illuminating light, and the correlation between absorption and wavelength results in a profile of the PA spectrum that is similar to the absorption spectrum. The PA amplitude signal also depends on the amount of absorbed energy converted into heat through non-radiative relaxation processes, and the phase behavior of the PA signal can be used to provide information related to the non-radiative relaxation time and thermal properties of the sample.

Spectra were subjected to second-derivative and curve-fitting procedures (Byler and Susi 1986; Yang et al. 1985; Dong et al. 1990; Bugs et al. 2004, 2005, 2007) in order to fit the absorption band for all proteins in the region 240–320 nm with a Gaussian band shape, using ORIGIN package. In the second-derivative spectrum, the peak frequency of an absorbance is identical to the original peak frequency (Susi and Byler 1986) and the number of bands and their positions can be accurately determined, which, in combination with the curve-fitting methods yields the most information of complex spectra (Maddams 1980). The wavelengths of the band center thus measured were used as initial input parameters for the band-fitting procedures. The procedure was in general carried out using only components detected by second derivative spectra after these had been considered and had their wavelengths fixed at these values. The fractional areas of the bands in the near UV region were calculated from the final fitted band area. Fitting was judged acceptable when the value of χ^2 was less than 10^{-6}.

Results and discussion

Figure 1 gives the original PA spectrum and shows the curve-fitting of six proteins with well-known structures that contain a varied number of aromatic amino acids in the sequences. The bands are strongly overlapping in aromatic amino acid region; resolution-enhancement is therefore required prior to analysis by curve-fitting procedures. The analysis of the amplitude signal in each protein was made first with the derivatives of the spectra and subsequent assigning of the position in the Gaussian band. The peak wavelengths of the second derivative spectra were used for the quantitative determination of the aromatic amino acid components in the protein by curve-fitting. After the Gaussian curve-fitting procedure the resulting component bands were assigned for all proteins in the same way. The curve-fitting shows five component peaks for LYS, OVA, and RSA; six peaks for BSA and BthTx-I and seven peaks for LGA. The second-derivative and the curve-fitting of the protein spectrum shows that the bands are in very similar positions to those assigned to the aromatic amino acids as described elsewhere (Creighton 1993). The mathematical solution to the decomposition of PA spectra in a sum of Gaussian bands with not restrictions was imposed on the initial band position. Some restriction not represents the real conformation of the aromatic amino acids in the protein structure because the position variations represent one condition of each amino acid in the structure and are different in each protein. The spectral shape is fitted by a sum of Gaussian bands. From the areas of these individual bands—after their assignment to the specific aromatic amino acid—their presence in the protein structure is calculated from their fraction of the total band area in the aromatic region. Thus, the results of this Gaussian area represent the contributions of each amino acid overlapping absorption bands. Although each protein will have a different aromatic composition and thus a different molar absorptivity, this method can accurately identify the contribution of each aromatic amino acid.

In order to analyze the contribution of the aromatic amino acid on the PA spectrum it is necessary to consider the radiative and nonradiative pathways of the decay in the excited state. This treatment of the data differentiates

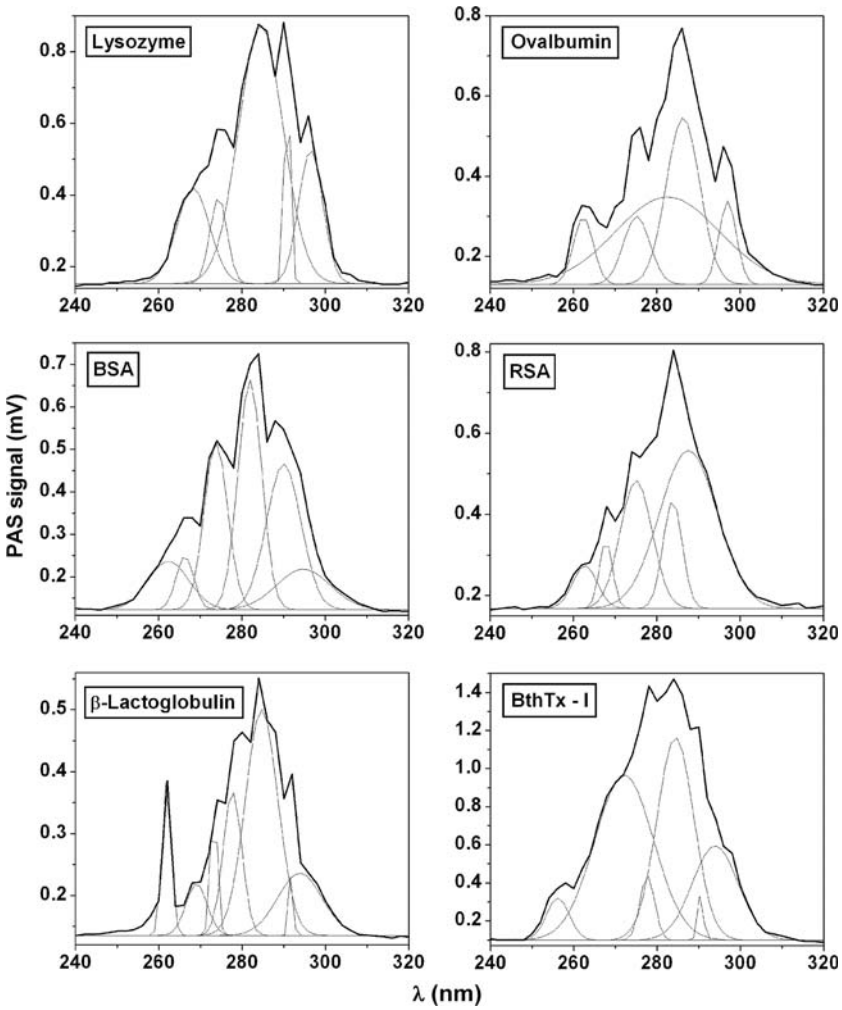

Fig. 1 Photoacoustic spectra of proteins in the near UV region. Band decomposition of the original absorption spectrum in Gaussian bands in order to obtain an estimate of the contribution of the aromatic amino acids in different proteins. The graphs include the original spectra and the five, six, and seven main Gaussian bands that compose the spectrum of each protein. The relative area of the Gaussian band has been given the percentage of each amino acid and the Gaussian errors are between 3 and 5%. The numerical values obtained are reflected in Table 1

PAS from conventional spectroscopic techniques, since, although the incident energy is in the form of electromagnetic radiation, the interaction with the sample under investigation is studied not through subsequent detection and analysis of a fraction of the photons, but rather through a direct measurement of the energy absorbed by the sample as a result of its interaction with the photon beam. The sample is illuminated with monochromatic light and, if any of the incident photons are absorbed by the sample, internal energy levels within the sample are excited. Upon subsequent relaxation of these energy levels, all or part of the absorbed photon energy is then transformed into heat energy through non-radiative relaxation processes (Bugs and Cornélio 2001, 2002). For this reason, the profile of the PA spectrum is similar to that obtained by absorption but not necessarily coincident with the absorption spectrum. The near UV absorption of tryptophan is dominated by two overlapping π–π^* transitions denominated as ^1L_a and ^1L_b (Valeur and Weber 1977), and in the case of tryptophan, the fluorescence involves both of these excited states. Energetically, ^1L_b lies above ^1L_a and is therefore excited predominantly at 280 nm, whereas ^1L_a is excited predominantly at 300 nm. The ^1L_a transition is sensitive to the polarity, giving rise to a slight shift in absorbance spectrum, and is believed to be the main contributor to the emission (Lakowicz 1999). This would imply that, when excitation is performed at 300 nm, only the tryptophan PA signal is observed. When excitation is performed at 280 nm, where both tyrosine and tryptophan absorb light, the PAS absorbance is derived from the two types of residues.

The heat generated by the PA effect from the aromatic amino acid needs a finite time to diffuse to the sample surface and generate the acoustic signal. This time delay has components that are derived from both the non-radiative relaxation and the thermal diffusion. The contribution of each absorption center to the PA signal can be considered to be derived from a spatially homogeneous distribution, since only light absorbed within the first thermal diffusion length contributes to the acoustic signal (in our experiments, 10 Hz modulation generated a diffusion length of 0.0066 cm—see for further details Bugs and

Cornélio (2001, 2002). Thus, any time lag in the PA signal may be attributed to the difference in the nonradiative relaxation times between the absorption centers.

Table 1 lists the band components and the peak positions, with the percentage area in each wavelength obtained for the aromatic amino acid components after curve-fitting of the six proteins. The numbers in the table represents the relative contribution of each aromatic amino acid in the PAS absorbance (non-radiative decay), as defined by previous location in function of molar absorptivities and the numbers of each amino acid in the protein. Complementary subdivision (gray in Table 1) have been made in respect of the relative molar extinction coefficients for each amino acid (Creighton 1993) in the Gaussian area, which helps the interpretation of the PA absorbance spectra in these regions with a percentage contribution to each aromatic in this peak wavelength. For LYS and LGA, the strong band centered at 284 nm is characteristic of tryptophan and received the major area in the curve-fitting. In the OVA the most intense band is 282 nm, inasmuch as BSA has two bands with almost the same intensity at 282 and 290 nm, RSA at 288 nm and BthTx-I at 272 nm. Since tyrosine does not absorb at wavelengths greater than 295 nm (Creighton 1993), the components above this are associated

Table 1 Values corresponding to percentage area obtained with a Gaussian fit on photoacoustic spectra of proteins

Lysozyme (LYS) (6W 3Y 3F)							
λ (nm)	268	274	284	290	296		
Gaussian area	15.14	7.18	55.78	6.18	15.72		
% to each amino acid	W = 13.42	W = 7.12	W = 52.50	W = 6.18	W = 15.72		
	Y = 1.72	Y = 0.06	Y = 3.28				
Ovalbumin (OVA) (3W 10Y 20F)							
λ (nm)	262	275	282	286	296		
Gaussian area	6.94	9.36	47.16	28.98	7.56		
% to each amino acid	W = 3.94	W = 5.02	W = 28.30	W = 22.80	W = 7.56		
	Y = 2.14	Y = 4.34	Y = 18.86	Y = 6.18			
	F = 0.86						
Bovine serum albumin (BSA) (3W 21Y 30F)							
λ (nm)	262	266	274	282	290	294	
Gaussian area	10.16	4.86	20.10	27.94	25.76	11.18	
% to each amino acid	W = 4.12	W = 1.77	W = 7.14	W = 11.64	W = 22.02	W = 11.18	
	Y = 4.70	Y = 2.72	Y = 12.96	Y = 16.30	Y = 3.74		
	F = 1.34	F = 0.37					
Rabbit serum albumin (RSA) (2W 25Y 28F)							
λ (nm)	262	268	275	284	288		
Gaussian area	6.12	5.20	23.70	12.00	52.98		
% to each amino acid	W = 1.75	W = 1.24	W = 5.59	W = 4.68	W = 37.67		
	Y = 3.57	Y = 3.96	Y = 18.11	Y = 7.32	Y = 15.31		
	F = 0.80						
β-Lactoglobulin A (LGA) (2W 4Y 4F)							
λ (nm)	262	268	274	278	284	292	294
Gaussian area	6.62	8.48	5.48	16.33	44.64	1.75	16.70
% to each amino acid	W = 4.76	W = 5.61	W = 3.61	W = 11.55	W = 35.71	W = 1.69	W = 16.7
	Y = 1.55	Y = 2.87	Y = 1.87	Y = 4.78	Y = 8.93	Y = 0.06	
	F = 0.31						
Bothropstoxin-I (BthTx-I) (1W 9Y 2F)							
λ (nm)	256	272	278	284	290	294	
Gaussian area	4.03	41.43	4.03	30.18	1.19	19.14	
% to each amino acid	W = 1.85	W = 11.77	W = 1.41	W = 14.21	W = 1.19	W = 19.14	
	Y = 1.96	Y = 29.66	Y = 2.62	Y = 15.97			
	F = 0.22						

The aromatic amino acids are represented by W, tryptophan; Y, tyrosine; F, phenylalanine

with absorption of the tryptophan (transition ^1L_a). Other bands also can be seen and connected with a contribution both to tyrosine and phenylalanine. The numbers of aromatic amino acid disagree in the position on the structure of proteins and the differences found in the Gaussian area translate the structure-function concept of each protein. The photophysics of these energy levels through non-radiative relaxation processes in each protein represents an amazing characteristic that reflects the chemical and molecular evolution.

In order to gain further insights into the changes in the bands of the aromatics environment, we conducted the interaction of SDS with BthTx-I, with the purpose of identifying the aromatic amino acids that participate in the interaction as previously observed during titration with SDS (Bortoleto-Bugs et al. 2004). The BthTx-I contains a single tryptophan residue at position 77 that is located at the dimer interface, the nine tyrosine residues are primarily located on the surface of the protein that makes contact with the lipid membrane and the two-phenylalanine residues are located in the N-terminal alpha helix and C-terminal loop regions respectively, yet the phenylalanine residue in the N-terminal helix is located closer to the dimer interface (da Silva Giotto et al. 1998). Figure 2 displays the spectra of BthTx-I protein in addition of SDS in a molar ration between 0 and 14 together with the curve-fitting in the aromatic region that provides an insight into function of the interaction in the Gaussian bands marked for each amino acid. A quantitative analysis of the PA spectra clearly shows changes in the energy levels of the aromatics caused by the SDS, and a comparison of these Gaussian bands may therefore enable us to analyze the dynamic interaction of the complex formed between SDS and BthTx-I, and allow us to make inferences about the contribution of different regions of the protein to the interaction. The curve-fitting presented in Fig. 2 was highly consistent and could be assigned to specific interactions or local environment alterations upon the addition of SDS, and have been assigned to the aromatic amino acids as previously described (Creighton 1993). The second derivatives on the native BthTx-I show peaks that have final fitted major band areas located at 272 nm (54% of Y and 46% of W) and 284 nm (63% of W and 37% of Y). Clear changes in the BthTx-I spectra were observed as SDS was increased. The second derivative spectra indicate that one or more amino acid residues are sensing changes resulting from the presence of SDS. Upon the addition of the two initial molecules of SDS changes were observed in the peaks with a significant increase in the Gaussian area at 290 nm that can be assigned to W, likewise heat was generated in the area of F region. With the binding of four molecules of SDS the contribution in the region assigned to pure W (292 nm) was maintained and it was also can possible to observe heat generated in the F and Y regions. With six molecules of SDS there was a reasonable distribution of the areas in the spectral region with a significant contribution in the 266 nm peak that gives evidence of a more prominent interaction in the W and Y regions. At SDS/protein ratio of 8, the interaction leads to a pure contribution of W (290 nm). The 10 molecules of SDS cause a large increase in the area at wavelengths around 300 nm, permitting an evaluation of the contribution of SDS interaction with BthTx-I in the tryptophan region (transition ^1L_a). The final fitted band areas, at 12 SDS, display an accentuated contribution of W and distinct Y. Binding of 14 SDS shows a more variable response to the addition of SDS with a large Gaussian band that indicates a heat generation distributed throughout the protein. Alternatively, these data may be interpreted as resulting from an alteration in the heat capacity of the SDS/protein complex as compared to the free protein in solution. Recent studies on the hydration of proteins suggest that the structure of the water that participates in the immediate hydration sphere is significantly altered in comparison to the bulk solution (Prabhu and Sharp 2006), which results in a significant contribution to the heat capacity of the protein/solvent system (Prabhu and Sharp 2005). On binding SDS, it is likely that this hydration sphere will be perturbed, altering the heat capacity of the system, and thereby modulating the transfer of heat from the vicinity of the tyrosine residues in the protein to the bulk solvent. For molar ratios above 10, the complex developed a significant light scattering, accompanied by a decrease in the intrinsic tryptophan fluorescence intensity emission (ITFE) of the protein (Bugs et al. 2007). Concomitantly, the near UV-PAS signal increased, confirming the predicted inverse relationship between ITFE and PAS intensities. The second derivative and curve-fitting procedures of PAS changes at SDS/BthTx-I ratios below 8 were limited to the 280–290 nm region, suggesting initial SDS binding to the tryptophan located in the dimer interface, together with the participation of phenylalanine residues in the relaxation process at the initial 2–4 molecules of SDS. Nevertheless, these results and interpretations are in close agreement with previous results (Bugs et al. 2007).

In summary, we report here an unusually spectroscopic characterization of aromatic amino acids in proteins. Here we have obtained additional insights into the formation and dynamics of the interaction between SDS and BthTx-I using PAS, demonstrating the capacity of this method to identify distinct binding modes of SDS to the protein which are not readily detectable by other techniques. These results demonstrate the potential of PAS for the study of the interaction processes of small molecules with proteins, and may be particularly useful for the investigation of those systems in which light scattering is predominant, such as

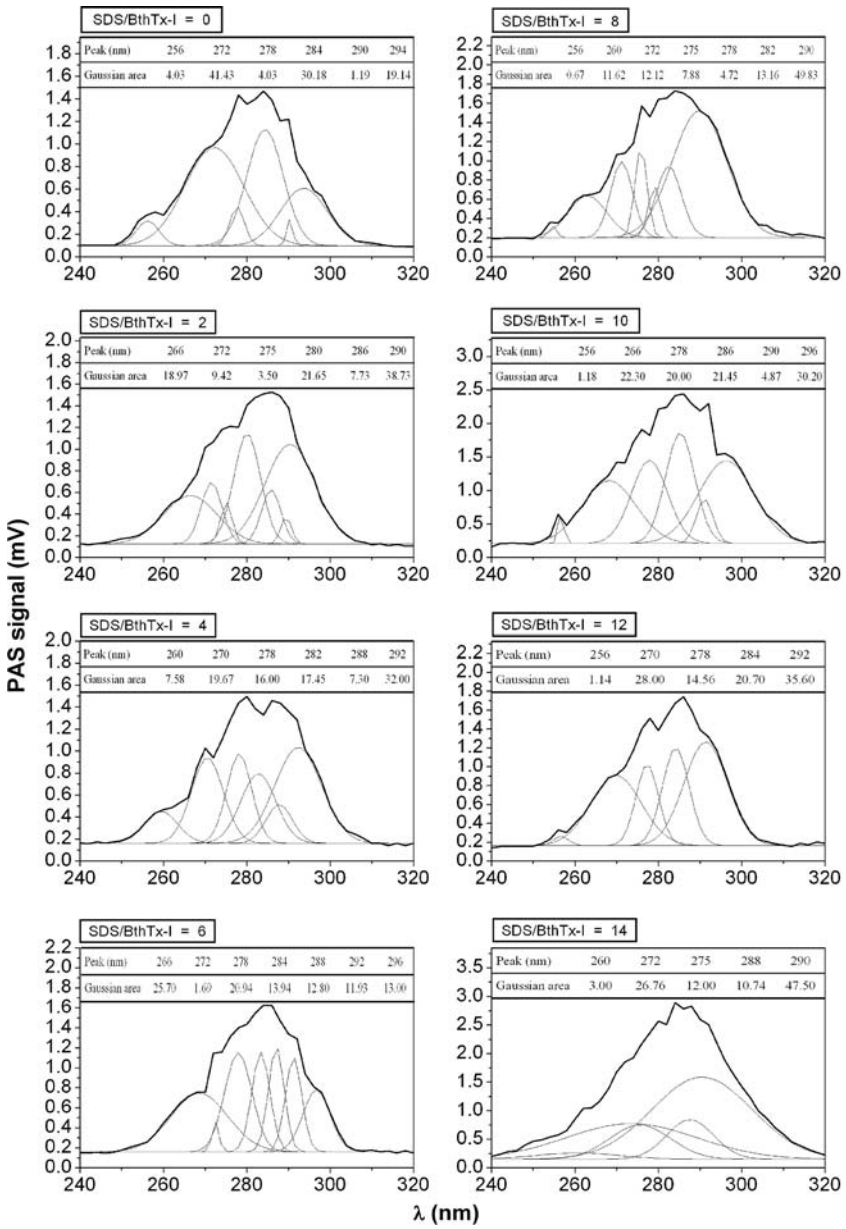

Fig. 2 PAS absorbance spectra in the aromatic region (240–320 nm) and their Gaussian curve-fitting of the BthTx-I with SDS. Assignment and fractional area (%) of the component bands were obtained by second-derivative resolution and Gaussian curve-fitting analysis (see text). Correlation coefficient varied between 0.994 and 0.998, and the Gaussian errors are between 3 and 5%

structure–function relationships of membrane proteins. Overall we demonstrate effectively that PAS can be used to obtain near UV spectra of proteins and that it is sensitive to changes in the protein conformation or environment.

Acknowledgments This research was supported by grants from the Fundação de Amparo a Pesquisa do Estado de São Paulo, FAPESP, MRB (96/07843-6), RKB-B (97/02749-4) and MLC (95/5038-6). MRB and RKB-B are indebted to Petróleo Brasileiro S.A. – PETROBRAS/Cenpes/Cognitus Project.

References

Abbruzzetti S, Crema E, Masino L, Vecli A, Viappiani C, Small JR, Libertini LJ, Small EW (2000) Fast events in protein folding: structural volume changes accompanying the early events in the N→I transition of apomyoglobin induced by ultrafast pH jump. Biophys J 78:405–415

Adams MJ, Highfield JG, Kirkbright GF (1977) Determination of absolute fluorescence quantum efficiency of quinine bisulfate in aqueous medium by optoacoustic spectrometry. Anal Chem 49:1850–1852

Adams MJ, Highfield JG, Kirkbright GF (1980) Determination of the absolute quantum efficiency of luminescence of solid materials employing photoacoustic spectroscopy. Anal Chem 52:1260–1264

Bortoleto-Bugs RK, Neto AA, Ward RJ (2004) Activation of Ca^{2+}-independent membrane- damaging activity in Lys49–phospholipase A2 promoted by amphiphilic molecule. Biochem Biophys Res Commun 322:364–372

Bugs MR, Cornélio ML (2001) Analysis of the ethidium bromide bound to DNA by photoacoustic and FTIR spectroscopy. Photochem Photobiol 74:512–520

Bugs MR, Cornélio ML (2002) A new biophysics approach using photoacoustic spectroscopy to study the DNA-ethidium bromide interaction. Eur Biophys J 31:232–240

Bugs MR, Forato LA, Bortoleto-Bugs RK, Fischer H, Mascarenhas YP, Ward RJ, Colnago LA (2004) Spectroscopic characterization and structural modeling of prolamin from maize and pearl millet. Eur Biophys J 33:335–343

Bugs MR, Bortoleto-Bugs RK, Cornelio ML (2005) The interaction between heparin and Lys49 phospholipase A2 reveals the natural binding of heparin on the enzyme. Int J Biol Macromol 37:21–27

Bugs MR, Bortoleto-Bugs RK, Cornélio ML, Ward RJ (2007) An ultraviolet photoacoustic spectroscopy study of the interaction between Lys49–phospholipase A2 and amphiphilic molecules. Biochem Biophys Res Commun 353:889–894

Byler DM, Susi H (1986) Examination of the secondary structure of proteins by deconvolved FTIR spectra. Biopolymers 25:469–487

Cornélio ML, Sanches R (1994) The use of photoacoustic spectroscopy to determine the critical distance for electron transfer. J Biochem Biophys Methods 29:149–155

Cornélio ML, Sanches R (1995) Monitoring electron transfer by photoacoustic spectroscopy. Eur Biophys J 23:439–442

Creighton TE (1993) Proteins structures and molecular properties. WH Freman and Company, New York, pp 14–17

da Silva Giotto MT, Garratt RC, Oliva G, Mascarenhas YP, Giglio JR, Cintra AC, de Azevedo Jr WF, Arni RK, Ward RJ (1998) Crystallographic and spectroscopic characterization of a molecular hinge: conformational changes in bothropstoxin I, a dimeric Lys49-phospholipase A2 homologue. Proteins 30:442–454

Dong A, Huang P, Caughey WS (1990) Protein secondary structures in water from second- derivative amide I infrared spectra. Biochemistry 29:3303–3308

Fork DC, Herbert SK (1993) The application of photoacoustic techniques to studies of photosynthesis. Photochem Photobiol 57:207–220

Kurian E, Prendergast FG, Small JR (1997) Photoacoustic analysis of proteins: volumetric signals and fluorescence quantum yields. Biophys J 73:466–476

Lahmann W, Ludewig HJ (1977) Opto-acoustic determination of absolute quantum yields in fluorescent solutions. Chem Phys Lett 45:177–179

Lakowicz JR (1999) Principles of fluorescence spectroscopy. Kluwer Academic/Plenum Publishers, New York

Maddams WF (1980) The scope and limitations of curve fitting. Appl Spectrosc 34:245–267

Malkin S, Cahen D (1979) Photoacoustic spectroscopy and radiant energy conversion: theory of the effect with special emphasis on photosynthesis. Photochem Photobiol 29:803–813

Mandelis A (1982) Photoacoustic determination of the non-radiative quantum efficiency of uranyl formate monohydrate, $UO_2(HCOO)_2 \cdot H_2O$, powders. Chem Phys Lett 91:501–505

Perkampus HH (1992) Recent developments in UV-VIS spectroscopy. In: Perkampus HH (ed) UV-VIS spectroscopy and its applications. Springer, Berlin, pp 101–120

Prabhu NV, Sharp KA (2005) Heat capacity in proteins. Annu Rev Phys Chem 56:521–548

Prabhu NV, Sharp KA (2006) Protein-solvent interactions. Chem Rev 106:1616–1623

Quimby RS, Yen WM (1980) Photoacoustic measurement of the ruby quantum efficiency. J Appl Phys 51:1780–1872

Rosencwaig A (1980) Photoacoustics and photoacoustics spectroscopy. John Wiley & Sons, New York

Valeur B, Weber G (1977) Resolution of the fluorescence spectrum of indole into the ^1L_a and ^1L_b excitation bands. Photochem Photobiol 25:441–444

Vladescu ID, McCauley MJ, Rouzina I, Williams MC (2005) Mapping the phase diagram of single DNA molecule force-induced melting in the presence of ethidium. Phys Rev Lett 95(15):158102

Yang WJ, Griffiths DM, Byler DM, Susi H (1985) Protein conformation by infrared spectroscopy: resolution enhancement by Fourier self-deconvolution. Appl Spectrosc 39:282–287